Detection of a Buried Horizon with a High Thermal Diffusivity Using Thermal Remote Sensing

*David B. Nash**
Jet Propulsion Laboratory 183-501, California Institute of Technology, Pasadena, CA 91109

ABSTRACT: The presence of a buried horizon with high thermal diffusivity may have a small but measurable effect on the temperature of the ground surface. If the overlying material is alluvium and the buried horizon is granite, modeling suggests that, for alluvium thicknesses of 1 m, the surface temperature of the alluvium underlain by granite may be as much as 0.2°C cooler at the peak of the summer heating cycle than adjacent areas not underlain by the granite. Vegetation, rain, and ground moisture will destroy or greatly attenuate this temperature contrast.

A field investigation was made in Upper Johnson Valley, Mojave Desert, California, an extremely arid region with abundant exposed or thinly buried low relief bedrock surfaces. A linear, anomalously cool area was observed to cross an alluvial surface in thermal imagery acquired immediately before dawn, 20 August 1982. The thermal anomaly was not associated with any topographic feature, change in vegetation, or albedo, and it ran perpendicular to the regional slope and the wind direction at the time the image was taken. The thermal diffusivity of the alluvium, measured *in situ* at the same time the image was acquired, did not vary between the anomaly and the adjacent area. Although it was initially assumed that the anomaly was due to the morphology of the buried bedrock, subsequent subsurface investigation suggests it was due to the presence of a *caliche* horizon 10 cm to 1 m below the surface having a thermal diffusivity nearly identical to that of granite.

The study suggests that thermal remote sensing provides an effective and relatively inexpensive means for detecting the presence of thinly veneered, high thermal diffusivity horizons. In extremely arid areas, it may be possible to detect buried bedrock topography and so delineate etched fault zones and buried channels capable of localizing groundwater circulation.

INTRODUCTION

THE TEMPERATURE of the ground surface is influenced by the thermal properties of the materials buried below it. Several workers, including Byrne and Davis (1980) and Nash (1985), have demonstrated that a layer with a high thermal diffusivity, κ ($\kappa = K/C$ where K is conductivity and C is volumetric heat capacity), overlain by a surface layer with a lower diffusivity, will decrease the amplitude of the diurnal and annual temperature cycles relative to that which would develop on an infinite thickness of the surface material alone. The effect of the underlying high diffusivity layer decreases rapidly with increasing depth of burial. For a given depth, the buried layer's effect on surface temperature will increase with an increase in the period of the heating cycle or with an increase in the thermal diffusivity of the buried layer.

A common example of the effect an underlying layer can have on surface temperature may be observed on the trunks of cars during clear, humid days in summer. In the evening, as the car trunk cools, water condenses where the surface temperature drops below the dew point. Portions of the trunk immediately above the support framework (high thermal diffusivity) cool more slowly than the surrounding unsupported areas. For a brief time, areas above the support framework are warm enough to be free of dew while the surrounding areas are not. The dew pattern, reflecting the surface temperature, shows the configuration of the underlying support framework even though the thermal properties of the sheet metal and paint are uniform over the surface of the trunk. When the sun comes up in the morning and the trunk heats up again, the areas above the support framework warm up more slowly than the surrounding areas so they retain their cover of dew longer and again the configuration of the support framework is visible, this time reflected by the dew-covered areas of the trunk.

Although detection of the configuration of the framework supporting the sheet metal of a car trunk is of no practical interest, detection of bedrock structures ($\kappa = 1.8 \times 10^{-2}$ cm^{2}s^{-1}) buried by a thin cover (less than 2 m) of alluvium ($\kappa = 3.2 \times 10^{-3}$ cm^{2}s^{-1}) is of considerable interest. In a previous paper (Nash, 1985), it is suggested that, at certain times during the annual heating cycle, the bedrock will cause the surface temperature of a 1-m thick cover of alluvium to differ by as much as 0.2°C from adjacent areas not underlain by bedrock (Figure 1). Alluvium underlain by bedrock will be slightly cooler during a several week long "window" in the summer and slightly warmer during a similar window in the winter. The timing of these windows is a complex function of depth of burial of the bedrock, the contrast in thermal properties of the alluvium and bedrock, and the amplitude and period of the heating cycle. The effect the buried bedrock exerts on the surface temperature of the overlying alluvium decreases rapidly with depth of burial, becoming negligible at depths exceeding 1.5 m (Figure 2).

For several reasons, the detection of alluvium veneered bedrock by thermal remote sensing is not feasible under any but the most severe desert conditions. Moisture in the alluvium will increase its thermal diffusivity to close to that of granite, decreasing the bedrock's effect on surface temperature. The near surface temperature profile can be "washed out" by a moderate rain. Vegetation masks the ground surface, making it difficult or impossible to measure soil brightness temperature by thermal remote sensing techniques.

Although thermal detection of buried bedrock may only be possible in deserts, there are extensive areas in the Mojave Desert and the Basin and Range of the southwest United States where alluvium thinly veneers bedrock, particularly in the vicinity of fault-generated mountain ranges. A remote sensing technique capable of detecting the topography of bedrock sur-

*Presently at the Department of Geology, University of Cincinnati, Cincinnati, OH 45221-0013.

PHOTOGRAMMETRIC ENGINEERING AND REMOTE SENSING,
Vol. 54, No. 10, October 1988, pp. 1437–1446.

0099-1112/88/5410–1437$02.25/0

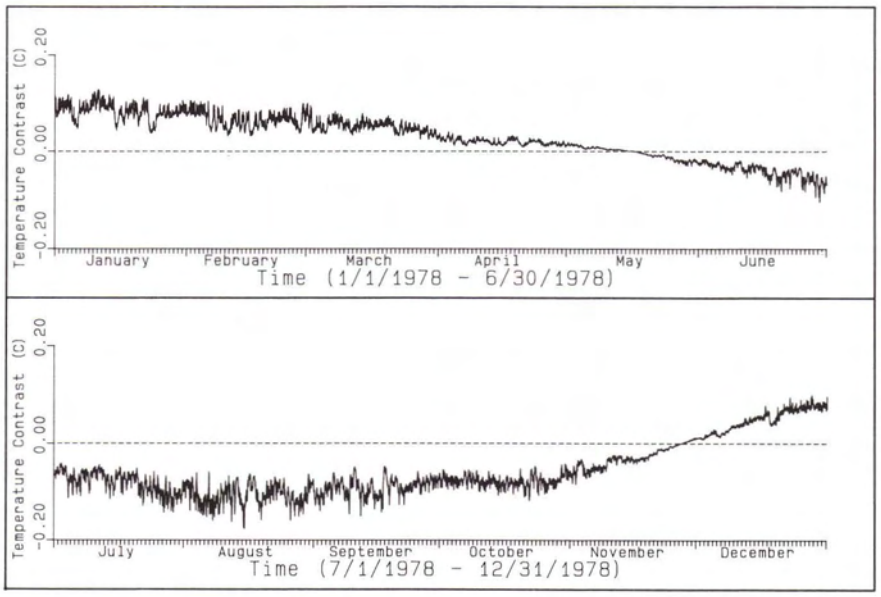

FIG. 1. Theoretical difference in surface temperature developed on a 1-m thick veneer of alluvium over an infinite thickness of granitic bedrock, T_v, and on an infinite thickness of alluvium alone, T_a. Temperature contrast is defined at $T_v - T_a$. During the summer, the alluvium veneered bedrock is a few tenths of a degree centigrade cooler, and during the winter it is a few tenths of a degree warmer than the alluvium alone (from Nash, 1985).

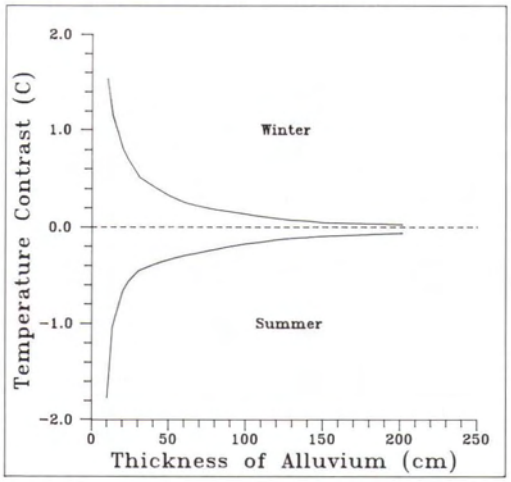

FIG. 2. Theoretical maximum surface temperature contrast between the alluvium veneered granitic bedrock, T_v, and an infinite thickness of alluvium alone, T_a, as a function of the thickness of the alluvium veneer. Temperature contrast is defined as $T_v - T_a$. The effect of the granitic bedrock on the surface temperature decreases rapidly with depth of burial (from Nash, 1985).

faces buried beneath a thin cover of alluvium would be a valuable tool for, among other things, locating range-front faults and other bedrock structures, and for delineating buried channels that may localize the flow of groundwater. The remote detection of buried bedrock topography by various means, particularly radar (e.g., Blom *et al.*, 1984), has been a subject of considerable interest.

The field investigation discussed here was undertaken to demonstrate the feasibility of detecting the surface topography of granitic bedrock beneath a thin cover of alluvium. A search was made for the optimal site in the most arid regions of the Mojave desert of California in areas where bedrock is bare or thinly veneered with alluvium. Such areas are called *pediments* or *suballuvial benches*. The way(s) in which these remarkably flat and areally extensive bedrock planes form has been a source of long standing and continued debate (Cooke and Warren, 1973). Some researchers ascribe their origin to the parallel retreat of mountain fronts, leaving a truncated bedrock surface in their wake (e.g., Lawson, 1915) while others (e.g., Oberlander, 1974) believe they form by stripping under desert conditions of a weathered mantle formed under more humid conditions in the past. Although the origin of pediments is not of direct importance to this study, it may well determine the types of features likely to be found on their surfaces.

STUDY SITE

Five well developed pediment surfaces in the Mojave Desert were examined. Of these, Upper Johnson Valley, on the northern flank of the San Bernardino Mountains (Figure 3), was found to be the most appropriate for study. The site is easily accessible; it is situated roughly midway between the towns of Lucerne Valley and Yucca Valley along California Route 287. The area is extremely arid with an annual precipitation of 10 to 20 cm falling primarily in the winter and with summer air temperatures reaching as high as 50°C. Because of the extreme aridity, the vegetation cover is remarkably sparse, even for the Mojave Desert, consisting primarily of creosote bush and thin grasses (Figure 4).

SURFICIAL GEOLOGY

Upper Johnson valley is a flat pediment surface studded with numerous spires of granitic bedrock. Between the granitic spires, the pediment surface is mantled by alluvium shed from the San Bernardino Mountains and from local bedrock highs. The alluvium, consisting primarily of pea size gravel and coarse sand, is locally overlain by *eolian* (i.e., wind blown) sand. This sand has a high albedo and is plainly visible in air photos as light,

FIG. 3. Portion of a Thematic Mapper 5 image (scene ID 50274-17520, band 4) of south-central Mojave Desert, California. The Upper Johnson Valley study site lies between two northwest trending granitic ranges that are fronted by northwest-striking, right-slip faults.

east trending streaks in the lee of bedrock spires on the *desert varnished* (dark colored coating of iron or magnesium oxide) alluvium (Figure 5A). The sand often accumulates to considerable thicknesses against the western flanks of ranges. A number of *playas*, dry lake beds filled only after heavy rains, are scattered through the area. The most notable, Means Lake, lies several kilometers north of the study site. In Upper Johnson Valley, the playas are floored with tan to red silts and clays. The playa surfaces have a higher albedo and moisture content than the surrounding alluvium.

BEDROCK GEOLOGY

Upper Johnson Valley is mapped on the Emerson Lake (Dibblee, 1967a) and Old Woman Spring (Dibblee, 1967b) 15° geologic quandrangle maps (Figure 6). The valley is flanked to the northeast and southwest by low, unnamed ranges. The ranges are linear, fault-fronted, and trend northwest-southeast as do several similar linear ranges in the area (Figure 3). The bedrock is Mesozoic diorites and monzonites with isolated outcrops of older, high grade metamorphic rocks.

FIG. 4. Ground level view of the Upper Johnson Valley study site looking southeast viewed from a granitic spire above tip of the eastern (right) arm of the "y" shaped thermal anomaly marked in Figures 5 and 6. The line of sight aligns exactly with the track of the anomaly which passes under the nearest "cottage" in the middle distance. No difference in surface albedo, vegetation cover, or topography is associated with the thermal anomaly.

The study site is crossed by the Johnson Valley fault and associated splays on the southwest and by a splay of Emerson fault on the northeast (Figure 6). Both faults are typical of the northwest-striking, right-slip faults that cut the Mojave Block into northwest-southeast trending slices. The structure of the area is complex and the mechanics of its formation are controversial (Garfunkel, 1974). On 15 March 1979, the area was jolted by a magnitude 5.2 earthquake, subsequently named the Homestead Valley Earthquake Swarm, which caused surface displacements, typically left-stepping *en echelon* tension cracks, in the alluvium (McJunkin, 1980; Stierman *et al.*, 1980; Hill *et al.*, 1980).

PREDICTED SUBALLUVIAL BEDROCK TOPOGRAPHY

The structure of the Upper Johnson Valley study site is strongly reflected in its topography. In fault zones, bedrock is highly fractured and exhibits slickensides. Epidote mineralization is common on fracture surfaces. Where they cross the pediment surfaces, the fault zones are presumably more erodible than the surrounding intact bedrock and should, therefore, be etched to form elongate furrows. If the surface of the overlying blanket of alluvium is flat, the etched furrow in the bedrock would cause local thickening of the alluvium over the fault. The greater depth to bedrock would cause the surface temperature of the thicker alluvium over the fault to be a few tenths of a degree warmer than surrounding areas during the summer heating maximum and a few tenths of a degree cooler than its surroundings during the winter heating minimum.

ACQUISITION OF THERMAL IMAGERY

Because no existing thermal imagery of the area was found to be appropriate for the study, it was decided to acquire predawn imagery in mid August, 1982. A flight was made at 0500 PDT (Pre-dawn) on 20 August 1982 using the NS001 Multispectral Scanner (an aircraft-borne version of the Landsat-D Thematic Mapper) aboard a C-130B. The NS001 instrument has a thermal spectral bandwidth of 10.4 to 12.5 μm, an instantaneous field of view of 2.5 mrad, and a noise equivalent $\triangle T$ of 0.25°C, and it records 699 pixels per scan line.

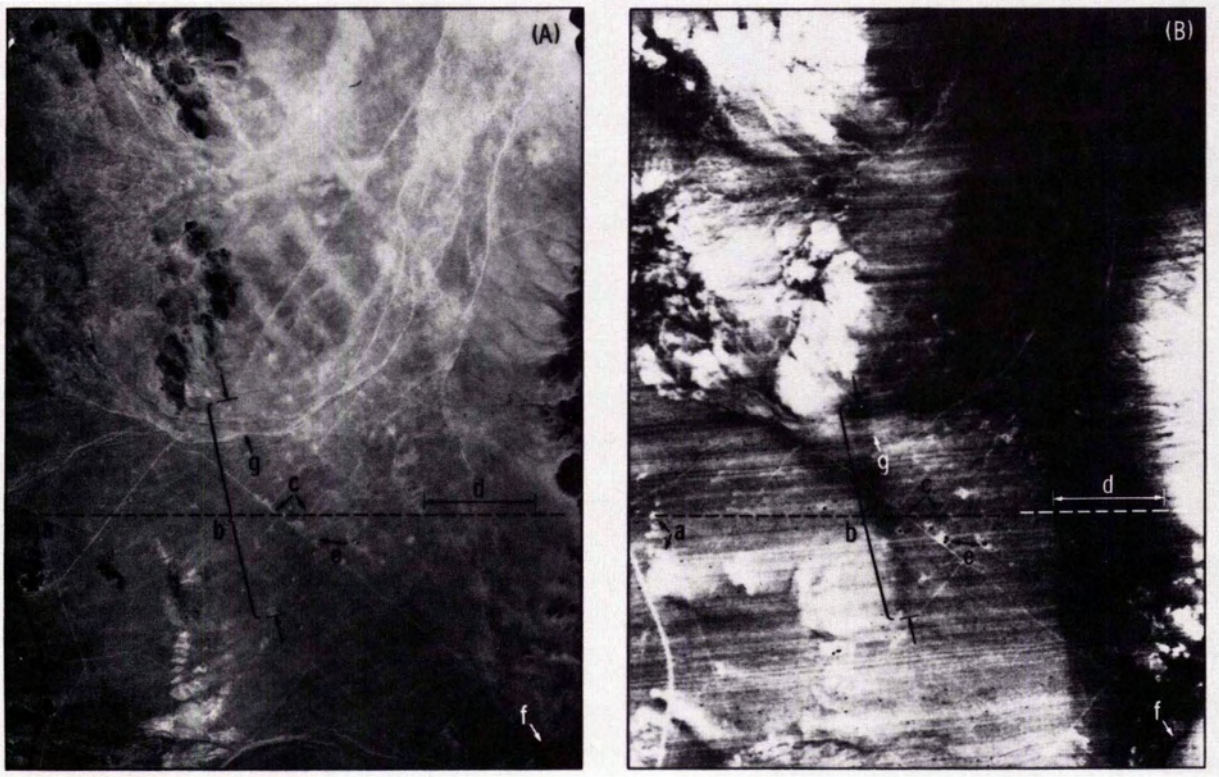

FIG. 5. (A) Portion of panchromatic air photo (U.S. Geologic Survey, project GS-VCMJ, Roll 1, Frame 52, taken 21 April 1970) covering the same area as mapped in Figure 6. (B) Image acquired by the thermal sensor (10.4 to 12.5 μm) of the NS001 Multispectral Scanner, an aircraft-borne version of the Landsat-D Thematic Mapper at 0500 PDT on 20 August 1982 from a height of 5200 m above the ground (sensor instantaneous field of view of, 2.5 mrad), is geometrically corrected using the air photo. Bedrock exposures, *a*, have a low albedo and are significantly warmer than surrounding alluvium covered areas in the pre-dawn thermal image. The thermal anomaly, *b* has no topographic expression (Figures 4 and 6) or difference in surface albedo associated with it. Dirt roads, *c*, have a higher albedo and night time temperature than the adjacent alluvium. The low wind speeds (Figure 12) may have allowed cool air to settle in topographic depressions, *d*. The roofs of homestead "cottages," *e*, (Figure 4) are cooler than the surrounding alluvium during the night. The small playa, *f*, has a higher albedo and is cooler than the surrounding alluvium. A deep (3 to 5 m) wash, *g*, cuts through the study area and across the thermal anomaly, revealing a caliche layer (Figure 11) beneath the anomaly. The dashed line corresponds to the path along which relative surface albedo and brightness temperature plots in Figure 7 were taken.

The aircraft altitude was 6100 m MSL (5200 m above the ground). Brightness temperatures were recorded as 8-bit words to the nearest quarter of a degree centigrade. The imagery was logged and corrected for edge distortion with the VICAR program C130RECX. An aerial photograph flown by the U.S. Geological Survey on 24 April 1970 (project number GS-VCMJ), roll 1, frame 52) was scanned and used to geometrically correct (register) the thermal image using the VICAR program MGEOM.

ANALYSIS OF THERMAL IMAGERY

The high thermal inertia ($\sqrt{KC}$) bedrock is clearly warmer than the adjacent alluvium in the pre-dawn thermal image. The tin roofed homestead "cottages" appear as black squares. The dirt roads appear warmer than the surrounding alluvium, probably because compaction has given them a higher thermal inertia and because they are free of vegetation. The eastern margin of the valley is cooler than the western margin, probably because it is topographically lower and ponds cool air (Figures 5 and 7).

An anomalous "y" shaped area, 0.2 to 0.4°C cooler than its surroundings, is visible on the eastern margin of the valley (Figures 5, 6, and 7). The west (left) arm of the "y" corresponds to a deep gully in which cool air may have been ponded, but the rest of the anomaly does not correspond to any obvious surface feature and is nearly perpendicular to the local slope (Figures 5 and 6). Although the east (right) arm and base of the "y" are to the east of the inferred trace of the Johnson Valley fault beneath the alluvium as mapped in Figure 6, the anomaly is a nearly straight line continuation of the trend of the fault in the bedrock immediately to the north.

THERMAL PROPERTIES OF THE ALLUVIUM

Five days before the overflight, four sample pits were dug at about 100-m intervals along a line perpendicular to the inferred location of the Johnson Valley Fault. Each pit was dug as rapidly as possible by hand to minimize the disturbance to the temperature profile. Thermistors where emplaced several centimeters into the walls of the pits and soil samples were taken for measurement of moisture content (Table 1). The pits were refilled with material in the same order in which it had been removed and the surfaces was restored, as much as possible, to its original appearance. The thermistors were read to the nearest 0.1°C at one- or two-hour intervals for the 24-hour period prior to the overflight.

After processing the imagery, sample pit T1H1 was found to lie to the east of the thermal anomaly, T1H2 was found to lie within the anomaly, and T1H3 and T1H4 were found to lie to the west of the anomaly. The thermal diffusivity of the alluvium in the sample pits was determined using an *in situ* technique derived from Van Wijk and DeVries (1963). The annual and diurnal surface temperature, T_0, may be approximated as a simple harmonic function of time, t, or

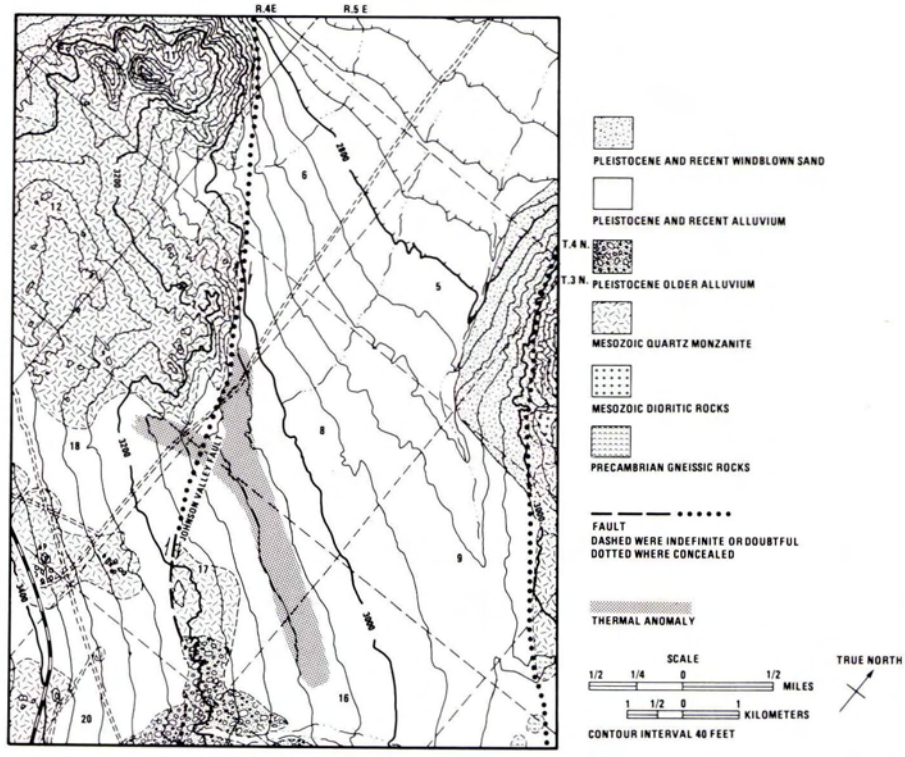

FIG. 6. Geologic map of the Upper Johnson Valley study site (from Dibblee, 1967a, 1967b) showing the location of the thermal anomaly visible in Fig. 5.

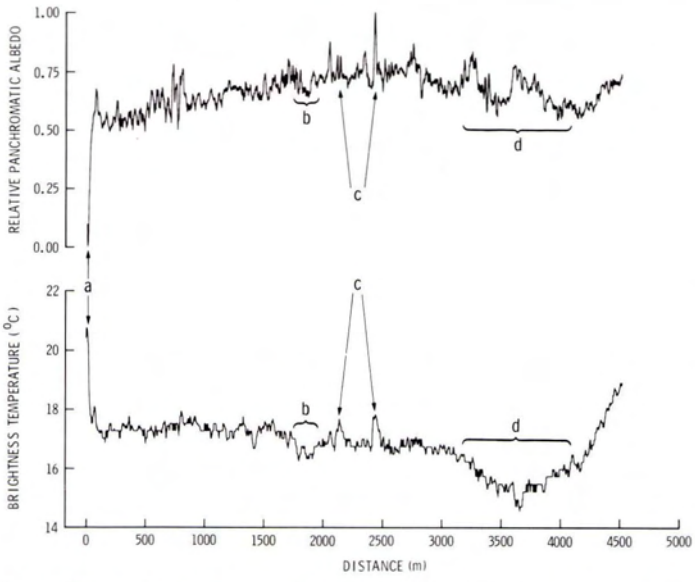

FIG. 7. Relative panchromatic albedo and brightness temperature measured from east to west along the dashed line in Figure 5 (*a* is exposed bedrock, *b* is the thermal anomaly, *c* are dirt roads in the alluvium, and *d* is a broad, shallow topographic depression.

$$T_0 = \overline{T} + A_0 \left[\frac{2t\pi}{P} + \phi \right] \tag{1}$$

where A_0 is amplitude, $\overline{T}$ is mean temperature, P is period (8.64×10^4s and 3.15×10^7s for the diurnal and annual cycle, respectively), and ϕ is phase. Assuming that the mean temperature, $\overline{T}$, is independent of depth, z, Van Wijk and DeVries (1963) prove that a one-dimensional diffusion model for heat transfer

$$\frac{\partial T}{\partial t} = \kappa \frac{\partial^2 T}{\partial z^2} \tag{2}$$

where κ is thermal diffusivity, results in a temperature T_z at a depth, z, described by

$$T_z = \overline{T} + A_z \sin \left[\frac{2t\pi}{P} + \phi - \phi_z \right] \tag{3}$$

where the cycle amplitude at depth z, A_z, is

$$A_z = A\, e^{-z/D}, \tag{4}$$

the phase shift, ϕ_z is

$$\phi_z = \frac{z}{D}, \tag{5}$$

and D, the thermal skin depth, is

$$D = \sqrt{\frac{\kappa P}{\pi}}. \tag{6}$$

TABLE 1. MOISTURE CONTENT OF ALLUVIUM

Sample Site	Depth (cm)	Moisture Content (%)
T1H1	0–5	0.00
T1H1	30	1.20
T1H1	62	1.32
T1H2	0–5	0.50
T1H2	40	6.06
T1H3	0–4	0.74
T1H3	30	1.01
T1H3	62	1.11

D may be determined by measuring the change in amplitude or phase of the temperature cycle at two different depths. If the amplitude of the cycle at depth z_1 is A_1 and its amplitude at depth z_2 is A_2, then

$$D = \frac{z_1 - z_2}{\ln(A_2/A_1)}. \quad (7)$$

Similarly, the phase difference between the temperature cycles at z_1 and z_2, $\triangle\phi_{2\text{-}1}$, may be used to determine D: i.e.,

$$D = \frac{z_1 - z_2}{\triangle\phi_{2-1}}. \quad (8)$$

Thermal diffusivity is determined from D with Equation 6.

The temperature profiles from the sample pits show the expected exponential decrease in diurnal temperature variation with depth (Figure 8). Because most of the heating of the surface is by solar radiation which does not vary sinusoidally with time (Kahle, 1977, her Figure 3), the temporal change in temperature measured by the thermistors near the surface can not be fit well by Equation 3. Below 5 cm, however, the temperature fluctuates nearly sinusoidally with time (Figure 9). The IBM Scientific Subroutine Package (IBM, 1968) procedure LLSQ is used to determine A_z and $\phi - \phi_z$ of the cycle that mostly closely fits the data for each thermistor. The average of the residuals, the absolute difference between observed temperature, and the temperature predicted by Equation 3, R_z, is determined for each thermistor. Thermistors whose heating cycles have an average ratio of R_z to A_z exceeding 0.2 are considered not to be described well by Equation 3 and are eliminated from the analysis. The average ratio of R_z to A_z for thermistors very close to the surface (less than 5 cm), where R_z is quite large, and for thermistors at depths greater than 40 cm, where A_z is quite small, exceeded 0.2 and thus these thermistors were not used to determine the thermal characteristics of the alluvium.

The near surface diffusivities observed in all the pits are about the same, 1-2 $\times$ 10^{-3} cm^2s^{-1} (Table 2). As will be the case for homogeneous materials, the decrease in $\ln(A_z)$ and $\phi - \phi_z$ with depth is approximately linear for T1H1 and T1H3. In T1H2, however, there is a sharp break in slope below 22 cm, indicating a significant increase in diffusivity (Figure 10, Table 2). This high diffusivity material differs markedly from the overlying alluvium and from that found in the other sample pits. Whereas the surrounding and overlying alluvium is tan colored, relatively course, and noncohesive, below 22 cm, the alluvium in T1H2 is brick red and highly cohesive, containing a significant amount of clay and silt with irregularly shaped blebs of carbonate. Although the word *caliche* is now avoided by soil scientists, it will be used here to refer to this highly calcified, clay-rich, red horizon.

The moisture content of alluvium taken at several depths from each sample pit was quite low, showing a slight increase with depth (Table 1). The moisture content was significantly higher for the caliche in T1H2, which might account, at least in part, for its higher diffusivity.

ANALYSIS

Subsurface Geology

The "y" shaped thermal anomaly correlates quite closely to the inferred position of the Johnson Valley Fault. It was expected, however, that the area above the fault would be *warmer* than its surroundings whereas the observed anomaly is *cooler* than its surroundings. If the observed anomaly is to be explained by thinly buried bedrock topography, then, contrary to expectation, the cover of alluvium must be *thinner* over the fault zone than over the surrounding area. Although it is not uncommon for mineralization, particularly silicification, of a fault zone to render it more resistant to weathering than the unfaulted rock, this is not the case for the fault zone in the exposed bedrock.

Several geophysical techniques were used to try to determine the morphology of the buried bedrock in the vicinity of the thermal anomaly. A twelve-channel, signal enhancing refracting seismograph was used with a sledge hammer source to

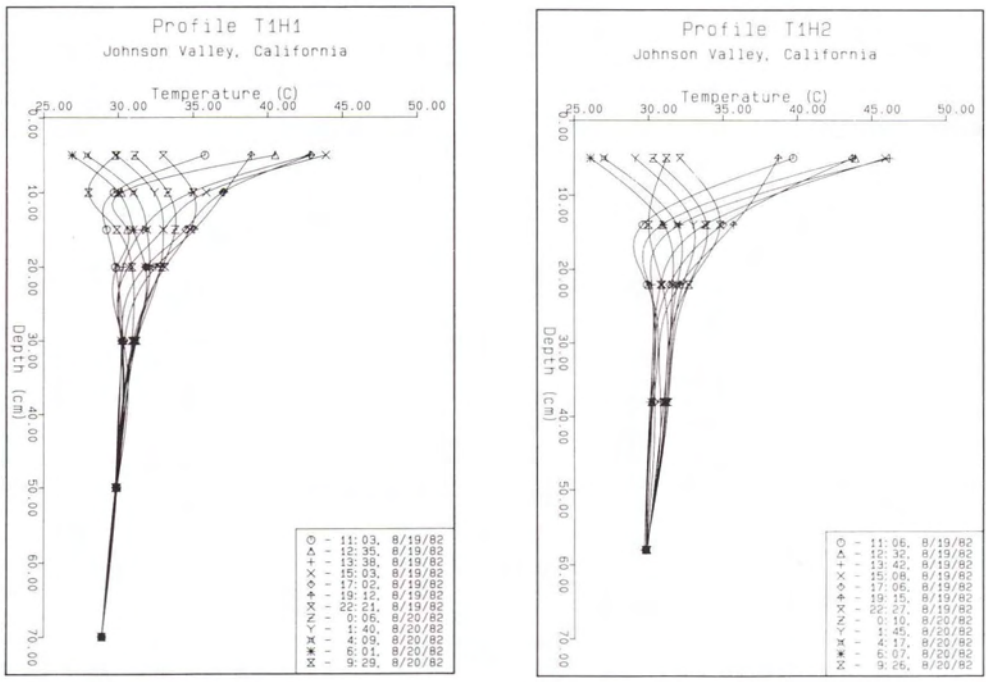

FIG. 8. Subsurface temperatures measured by arrays of thermistors buried at various depths in alluvium east of the thermal anomaly (T1H1) and within the thermal anomaly (T1H2).

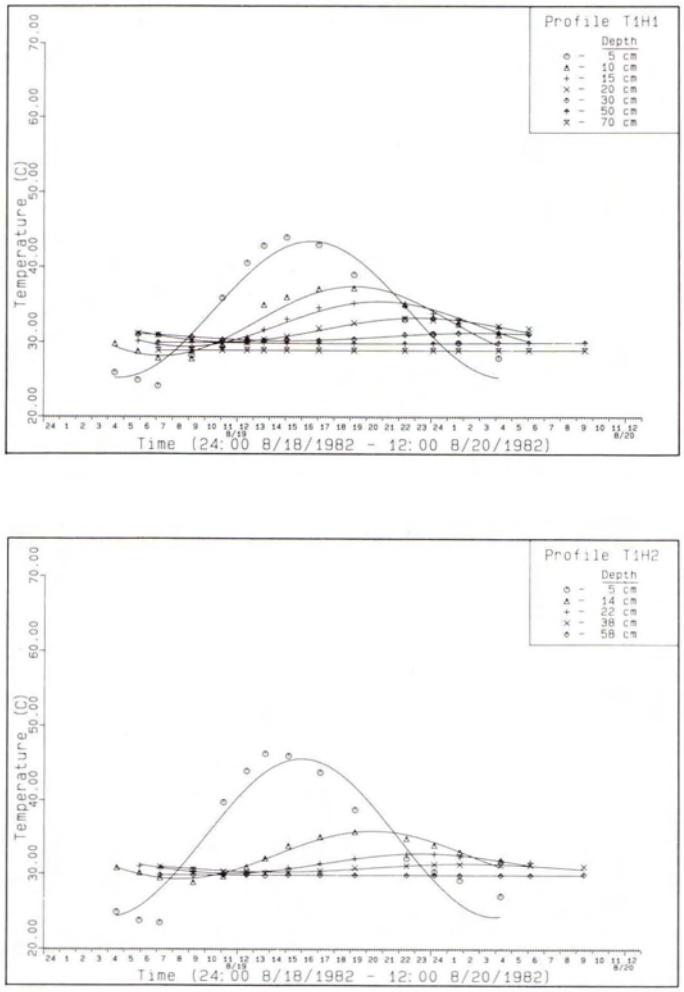

FIG. 9. The observed diurnal change in subsurface temperature at depths greater than 10 cm can be fit quite closely with a simple sinusoid (solid line). With increasing depth, there is a negative shift in the phase of the cycle, and its amplitude decreases. T1H1 is located to the east of the thermal anomaly and T1H2 is located within the anomaly.

TABLE 2. DIFFUSIVITY OF ALLUVIUM

Sample Site	Depth (cm)	Diffusivity (cm^2s^{-1})
T1H1	5–10	1.9×10^{-3}
T1H1	10–15	5.3×10^{-3}
T1H1	15–20	2.3×10^{-3}
T1H1	20–30	3.6×10^{-3}
T1H2	5–14	2.2×10^{-3}
T1H2	14–22	3.4×10^{-3}
T1H2	22–38	15.0×10^{-3}
T1H3	7–12	1.1×10^{-3}
T1H3	12–17	1.2×10^{-3}
T1H3	17–27	4.2×10^{-3}
T1H4	5–10	2.2×10^{-3}
T1H4	10–20	2.0×10^{-3}

determine the depth and slope of the bedrock along several traverses run perpendicular to the anomaly. No underlying unit was found with a seismic velocity high enough to be bedrock within the 10- to 15-m range of the seismograph.

The greater than anticipated thickness of the alluvium was subsequently confirmed by a series of borings using a truck mounted auger. Borings were made along three dirt roads that cross the anomaly. Holes were bored within the anomaly and on either side of it. Bedrock was not reached in any of the boreholes, some of which extended to a depth of 3 m. The borings did, however, encounter a brick red, highly calcified horizon similar to the caliche in pit T2H2 at depths from 20 cm to 1 m within the area of the thermal anomaly. This horizon was sufficiently indurated to be impenetrable to the auger. The association of the caliche with the thermal anomaly is quite clear in a deep (3- to 5-m) wash that cuts across the thermal anomaly (g in Figure 5). The caliche is observed in the walls of the wash only where it crosses the thermal anomaly. At several points along the wash, the horizon was highly calcified (Figure 11). The origin of the caliche is beyond the scope of this paper but it may be the same unit Sharp (1984) describes from a pipeline excavation approximately 40 km to the north of Upper Johnson Valley and which he names the Qa_2 Unit. He describes it as:

> . . . distinctive . . . owing to its reddish, dark brown color, rich clay content, soil structures, and coherence. Calcification is moderate and extends to the top of the reddish layer . . .. Locally the calcification has developed nodular form.

He later suggests:

> Its reddish color, considerable clay, and significant associated calcification indicate weathering of considerable duration or greater efficiency, probably both . . .. The reddish color of Qa_2 material presumably developed under more moist conditions than now exist . . ..

The auger operator was quite familiar with the unit. He had encountered it sporadically in borings for utility poles and supports for billboards and it had made augering difficult or impossible. Despite considerable experience, he had not found a reliable surface feature indicating the presence of the caliche in the subsurface; in his words, "Caliche's where you find it."

POSSIBLE CAUSES OF THERMAL ANOMALY

The observed anomaly is apparently not caused by a difference in surface albedo, soil moisture, or the thermal properties of the surface materials, nor could it be caused by buried bedrock topography because the bedrock's effect on surface temperature is negligible at burial depths of more than 1.5 m (Figure 2). A number of alternate explanations for the anomaly are possible, but most can be eliminated.

Cloud Tracks. The ground surface within the shadow cast by the slow passage of a cloud can result in surface temperatures cooler than its surroundings. It is unlikely that such anomalies would persist very long after sundown, certainly not until nearly dawn of the following day. The night of 19 August 1982 was cloud free. For these reasons, it is unlikely that the observed anomaly resulted from a cloud shadow.

Cold Air Ponding in Topographic Depressions. In the absence of wind, cool air will settle in topographic depressions. Wind speeds on the night of 19 August 1982 were quite low (Figure 12) so cool air ponding probably occurred. The western arm of the "y" shaped anomaly lies along a fairly wide and deep wash and may be due to this cause. The rest of the anomaly has no topographic expression and cuts perpendicularly across the slope and, therefore, could not be caused by cool air ponding.

Wind Streaks. Topographic obstructions divert or concentrate the wind on the ground surface. This may result in temperature streaking of the surface in a direction parallel to the wind direction. The winds on the night of 19 August 1982, however, were quite light and nearly perpendicular to the thermal anomaly.

Sand Streaks. Elongate accumulations of sand deflated from playas frequently accumulate in the lee of bedrock obstructions in the arid basins of the Mojave desert. Because the sand has a higher albedo then the adjacent alluvium, these streaks of sand are usually visible (north-central portion of the Upper Johnson

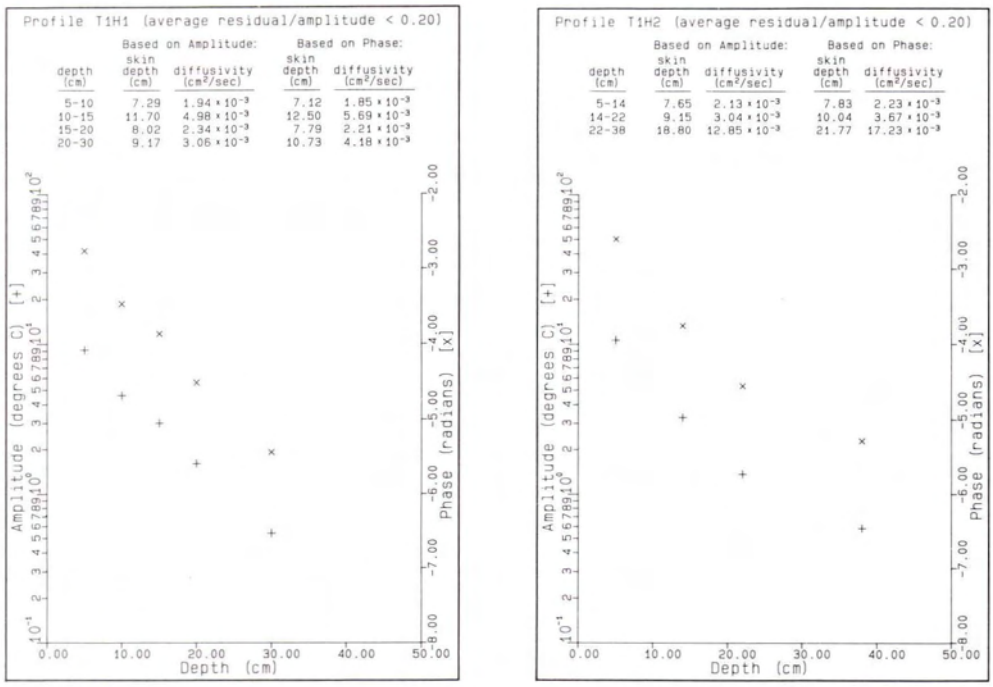

FIG. 10. The change in amplitude or phase of the temperature cycle with depth can be used to calculate the thermal diffusivity of the alluvium between two adjacent thermistors. Although the near-surface thermal diffusivities of the alluvium to the east of the thermal anomaly (T1H1) and within the thermal anomaly (T1H2) are nearly identical, the calcified horizon, encountered at 22 cm in T1H2, has a diffusivity four times higher than the uncalcified alluvium at an equivalent depth in T1H1.

FIG. 11. Calcified soil horizon (caliche) found to underlie the thermal anomaly visible in Figure 5. This horizon was encountered in borings and was visible on the sides of the deep wash (*g* in Figure 5) which cuts across the anomaly. The depth to this horizon varied from 20 cm to 1 m.

Valley study area, Figure 5). Sand generally has a lower thermal inertia than alluvium and, therefore, the night time surface temperature of accumulations of sand may be cooler than the adjacent alluvium surface. It is highly unlikely, however, that the thermal anomaly could be caused by a sand streak. No sand streaks in the vicinity of the anomaly are visible in air photographs (Figure 5) nor on the ground surface (Figure 4). In addition, none of the sand streaks visible in the panchromatic image in Figure 5 has a measurable effect on the brightness temperature of the surface. The orientation of the visible sand streaks, presumably reflecting the prevailing wind direction, does not parallel the direction of the thermal anomaly.

Moisture. The presence of moisture can have a profound effect on surface and subsurface temperature by increasing the latent heat flux (if the surface soil is moist) and by increasing the effective thermal inertia of the soil to close to that of granite. A number of studies have investigated the feasibility of thermal prospecting for ground water, including Cartwright (1968), Birman (1969), Moore and Myers (1972), Myers and Moore (1972), Rosema (1976), and Huntley (1978).

The moisture content of the surface layer alluvium did not differ between the anomaly and the surrounding area (Table 1), so it is unlikely that the anomaly was caused by increased latent heat flux. The moisture content of the caliche layer in T1H2 was an order of magnitude greeter than that of the surrounding area not within the thermal anomaly. Whether the much higher thermal diffusivity associated with the caliche is due to its elevated moisture content or to some other thermal characteristic of the material, it could lower the surface temperature of the overlying alluvium as discussed in the following section.

High Diffusivity of Buried Caliche Layer. Whatever causes the over four-fold increase in the thermal diffusivity of the caliche layer compared with the adjacent and overlying alluvium, its diffusivity and, therefore, its effect on the surface temperature will be nearly identical to that of granitic bedrock. In late summer, a thick horizon with a thermal diffusivity of 1.5×10^{-2} cm^2s^{-1} buried by a 20-cm to 1-m depth of alluvium with a diffusivity

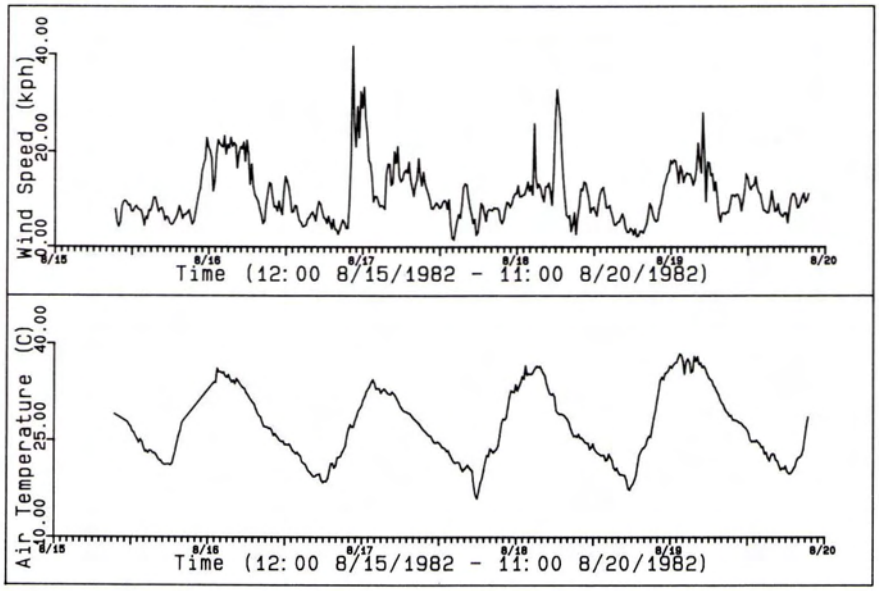

FIG. 12. Wind speed and air temperature measured at screen height by a portable, continuously recording, weather station located in the southeast corner of sec. 7, T. 3 N., R. 5 E. (Figure 6).

of $2.0 \times 10^{-3} cm^2 s^{-1}$ would be expected to cause surface temperatures 0.1 to 0.6°C cooler than adjacent areas not underlain by the horizon (Figure 2). The observed thermal anomaly was about 0.3 to 0.5°C cooler than the adjacent area, well within the range predicted by modeling studies. By the process of elimination, the presence of a buried horizon with a high diffusivity appears to be the most probable explanation for the anomaly.

CONCLUSION

This study suggests that a buried high thermal diffusivity horizon measurably lowers the surface temperature of the overlying lower diffusivity material during the peak of the annual heating cycle. The most likely explanation for the anomalously cool area is that the underlying caliche, having a much higher thermal diffusivity than the overlying and adjacent alluvium, acts as a local heat sink. This conclusion is reached by eliminating other possible causes for the anomaly.

Although tentative, the positive findings of this study suggest that additional studies should be made of the detectability of subsurface features using thermal remote sensing. A more convincing demonstration of how the presence of a buried high diffusivity material effects surface temperature could be made if a study similar to the one described here were undertaken of a suballuvial bedrock bench whose surface morphology is well known (an unsuccessful search was made for such a bench for this study). In addition, an investigation should attempt to find similar, anomalously warm areas over buried, high diffusivity materials during the winter. Despite the expense and difficulty of these studies, the benefits that would accrue from a reliable method for detecting shallow bedrock topography beneath a cover of alluvium would justify the effort.

ACKOWLEDGMENTS

This work was done while the author was a NASA-National Research Council Resident Research Associate at the Jet Propulsion Laboratory, California Institute of Technology, under the supervision of Dr. Anne B. Kahle. Dr. Robert P. Sharp (Caltech) suggested the study site and provided helpful advice during the course of the study. Dr. Kahle is thanked for her guidance, for sharing her thermal modeling expertise, and for providing the overflight of Upper Johnson Valley. Elsa Abbott, Michael Abrams, Alan Gillespie, Peg Hochhausler, Leon Maldonado, Helen N. Paley, and Earnie Paylor are thanked for their field assistance. The author particularly wishes to thank Mr. Frank D. Palluconi, who provided invaluable assistance both in the field and the laboratory. The research described in this paper was carried out by the Jet Propulsion Laboratory, California Institute of Technology, under contract with the National Aeronautics and Space Adminstration.

REFERENCES

Birman, J.H., 1969. Geothermal exploration for groundwater. *Geological Society of America Bulletin*, 80:617–630.

Blom, R.G., R.E. Crippen, and C. Elachi, 1984. Detection of subsurface features in Seasat radar images of Means Valley, Mojave Desert, California. *Geology*, 12:346–349.

Byrne, G.F., and J.R. Davis, 1980. Thermal inertia, thermal admittance and the effects of layers. *Remote Sensing of Environment*, 9:295–300.

Cartwright, K., 1968. *Temperature Prospecting for Shallow Glacial and Aluvial Aquifers in Illinois*. Illinois State Geological Survey Circular 433. Illinois Geological Survey, Urbana. 41p.

Cooke, R.V., and A. Warren, 1973. *Geomorphology in Deserts*, University of California Press, Berkeley, 394p.

Dibblee, T.W., Jr., 1967a. *Geologic Map of the Emerson Lake Quadrangle, San Bernardino County, California*. Miscellaneous Geologic Investigation Map I-490, U.S. Geologic Survey.

———, 1967b. *Geologic Map of the Old Woman Springs Quadrangle, San Bernardino County, California*, Miscellaneous Geologic Investigation Map I-518, U.S. Geologic Survey.

Garfunkel, Z., 1974. Model for the Late Cenozoic tectonic history of the Mojave Desert, California and for its relation to adjacent areas, *Geological Society of America Bulletin*, 85:1931–1944.

Hill, R.L., J.A. Treiman, J.W. Given, J.C. Pechmann, J.R. McMillan, and J.E. Ebel, 1980. Geologic study of the Homestead Valley earthquake swarm of March 15, 1979, *California Geology*, 33:60–67.

IBM Corporation, 1968. *System/360 Scientific Subroutine Package Version III, Programmer's Manual*, Program Number 360A-CM-03X, Manual GH20-0205-4. IBM Corporation: New York, 456p.

Kahle, A.B., 1980. Surface thermal properties. *Remote Sensing in Geology* (B.S. Siegal and A.R. Gillespie, eds). John Wiley and Sons, New York, pp. 257–273.

Lawson, A.C., 1915. The epigene profiles of the desert. *University of California Bulletin, Department of Geology*, 9:23–48.

McJunkin, R.D., 1980. Strong-motion data for the Homestead Valley earthquake swarm, San Bernardino County, California, 15 March 1979, *California Geology*, 33:11–13.

Moore, D.G., and V.I. Myers, 1972. *Environment Factors Affecting Thermal Groundwater Mapping*, Technical Report SDSU-RSI-72-06 for USFS Contract No. 14-08-001. Remote Sensing Institute, Brookings, 23p.

Myers, V.I., and D.G. Moore, 1972. Remote sensing for defining aquifers in glacial drift. *Proceedings of the Eighth International Symposium on Remote Sensing of Environment*, Environmental Research Institute of Michigan, Ann Arbor, pp. 715–728.

Nash, D.B., 1985. Detection of bedrock topography beneath a thin cover of alluvium using thermal remote sensing. *Photogrammetric Engineering and Remote Sensing*, 51:77–88.

Oberlander, T.M., 1974. Landscape inheritance and the pediment problem in the Mojave Desert of Southern California, *American Journal of Science*, 274:849–875.

Rosema, A., 1975. Simulation of the thermal behavior of bare soils for remote sensing purposes, *Heat and Mass Transfer in the Biosphere—Part I, Transfer Processes in the Plant Environment* (D.A. De Vries and N.H. Afghan, eds). John Wiley and Sons, New York, pp. 109–123.

Sharp, R.P., 1984. Alluvial microstratigraphy, Mojave Desert, *California Geology*, 37:139–145.

Stierman, D.J., Tien-Chang Lee, S.O. Zappe, and D. Seamount, 1980. Aftershocks of the Homestead Valley earthquakes of March 15, 1979, *California Geology*, 33:14–17.

Van Wijk, W.R., and D.A. De Vries, 1963. Sinusoidal temperature variations in layered soils, *Physics of Plant Environments* (W.R. Van Wijk, ed). John Wiley and Sons, New York, pp. 109–123.

(Received 27 December 1987; accepted 7 March 1988; revised 17 June 1988)

Forthcoming Articles

F. J. Ahern and *J. Sirois*, Reflectance Enhancements for the Thematic Mapper: An Efficient Way to Produce Images of Consistently High Quality.
Michael H. Brill and *James R. Williamson*, Multi-Sensor DLT Intersection for SAR and Optical Images.
Christopher W. Brown, Daniel L. Civco, and *William C. Kennard*, Adaptation of a Hand-Held Radiometer for Measuring Upwelling Radiance in the Aquatic Environment.
Jack Bryant, On Displaying Multispectral Imagery.
Pat S. Chavez, Jr. and *Jo Ann Bowell*, Comparison of the Spectral Information Content of Landsat Thematic Mapper and SPOT for Three Different Sites in the Phoenix, Arizona Region.
Liping Di and *Donald C. Rundquist*, Color-Composite Image Generation on an Eight-Bit Graphics Workstation.
S. A. Drury and *G. A. Hunt*, Remote Sensing of Laterized Archaean Greenstone Terrain: Marhall Pool Area, Northeastern Yilgarn Block, Western Australia.
Thomas D. Frank, Mapping Dominant Vegetation Communities in the Colorado Rocky Mountain Front Range with Landsat Thematic Mapper and Digital Terrain Data.
Tuomas Häme and *Markku Rantasuo*, Shuttered Camera — Aerial Color Video Imaging in the Visible and Near Infrared.
James A. Henry, Steven E. Dicks, Organ F. Wetterqvist, and *Stephen J. Roguski*, Comparison of Satellite, Ground-Based, and Modeling Techniques for Analyzing the Urban Heat Island.
Susanne Hummer-Miller, A Digital Mosaicking Algorithm Allowing for an Irregular Join "Line."
Peter A. Murtha and *Raoul J. Wiart*, Cluster Analysis of Pine Crown Foliage Patterns Aid Identification of Mountain Pine Beetle Current-Attack.
Paul G. Pilon, Philip J. Howarth, Ronald A. Bullock, and *Peter O. Adeniyi*, An Enhanced Classification Approach to Change Detection in Semi-Arid Environments.
Urho A. Rauhala, Compiler Positioning System: An Array Algebra Formulation of Digital Photogrammetry.
Urho A. Rauhala, Don Davis, and *Ken Baker*, Automated DTM Validation and Progressive Sampling Algorithm of Finite Element Array Relaxation.
Yang Shiren, Li Li, and *Gao Peng*, Two-Dimensional Seam-Point Searching in Digital Image Mosaicking.
E. Lynn Usery and *R. Welch*, A Raster Approach to Topographic Map Revision.
H. D. Williamson, The Discrimination of Irrigated Orchard and Vine Crops Using Remotely Sensed Data.
James R. Williamson and *Michael H. Brill*, Dominant Geometry Combinations of Two- and Three-Point Perspective in Close-Range Applications.

November 1988 Geographic Information Systems (GIS) Issue

G. F. Bonham-Carter, F. P. Agterberg, and *D. F. Wright*, Integration of Geological Datasets for Gold Exploration in Nova Scotia.
James R. Carter, Digital Representations of Topographic Surfaces.
David J. Cowen, GIS versus CAD versus DBMS: What Are the Differences? A Commentary.
Peter L. Croswell and *Stephen R. Clark*, Trends in Automated Mapping and Geographic Information System Hardware.
Andrew U. Frank, Requirements for a Database Management System for a GIS.
George F. Hepner, Thomas L. Logan, and *Nevin A. Bryant*, Spatial Query for Decision Support of Cross-Country Movement.
Michael E. Hodgson, John R. Jensen, Halkard E. Mackey, Jr., and *Malcolm C. Coulter*, Monitoring Wood Stork Foraging Habitat Using Remote Sensing and Geographic Information Systems.
S. K. Jenson and *J. O. Domingue*, Extracting Topographic Structure from Digital Elevation Data for Geographic Information System Analysis.
Carol A. Johnston, Naomi E. Detenbeck, John P. Bonde, and *Gerald J. Niemi*, Geographic Information Systems for Cumulative Impact Assessment.
H. Dennison Parker, The Unique Qualities of a Geographic Information System: A Commentary.
E. Lynn Usery, Phyllis Altheide, Robin R. P. Deister, and *David J. Barr*, Knowledge-Based GIS Techniques Applied to Geological Engineering.
Jan W. van Roessel, Conversion of Cartesian Coordinates from and to Generalized Balanced Ternary Addresses.